JOURNAL OF CHEMICAL & ENGINEERING DATA

ARTICLE

pubs.acs.org/jced

Kinetics and Isotherm Analysis of Basic Dyes Adsorption onto Almond Shell (*Prunus dulcis*) as a Low Cost Adsorbent

Celal Duran,*[,†] Duygu Ozdes,[†] Ali Gundogdu,[‡] and Hasan Basri Senturk[†]

[†]Department of Chemistry, Faculty of Sciences, Karadeniz Technical University, 61080 Trabzon, Turkey

[‡]Department of Food Engineering, Faculty of Engineering, Gümüşhane University, 29100 Gümüşhane, Turkey

ABSTRACT: The feasibility of using an agricultural byproduct, almond shell (*Prunus dulcis*), as an adsorbent in removal of basic dyes, namely, methylene blue (MB), methyl violet (MV), and toluidine blue O (TB), were evaluated in a batch adsorption process. The adsorption characteristics of MB, MV, and TB onto almond shell (AS) were investigated with respect to the changes in initial pH of dye solutions, contact time, initial dye concentration, and temperature. The dye adsorption equilibria were rapidly attained after 30 min of contact time. The adsorption kinetics were analyzed using pseudofirst-order, pseudosecond-order, Elovich, and intraparticle diffusion models and the adsorption data were well described by the pseudosecond-order model. The equilibrium adsorption data were interpreted in terms of the Langmuir, Freundlich, Temkin, and Dubinin−Radushkevich (D-R) isotherm models. The monolayer adsorption capacity of AS was found to be 51.02 mg·g^{-1} for MB, 76.34 mg·g^{-1} for MV, and 72.99 mg·g^{-1} for TB by using the Langmuir model equation. The thermodynamic parameters proved that the present adsorption process was feasible, spontaneous and endothermic in nature in the temperature range of (5 to 40) °C.

1. INTRODUCTION

The discharge of dyes and their break down products into receiving waters by many industries causes extremely toxic effects to aquatic life even at low concentrations.[1] In natural streams, dyes may inhibit the growth of biota, have a tendency to chelate metal ions that produce microtoxicity to fish and other organisms, and interfere with transmission of sunlight into streams hence reduce light penetration and photosynthetic activity.[2] Furthermore they may be mutagenic, teratogenic, and carcinogenic and cause many health disorders to human beings such as dysfunction of the kidney, reproductive system, liver, brain, and central nervous system.[3] Dyes can be classified as anionic (direct, acid, and reactive dyes), cationic (basic dyes), and nonionic (disperse dyes).[4]

The basic dyes are widely used to color silk, leather, plastics, and paper and also to produce ink and copying paper.[5] Because of the common utilization of these types of dyes in industrial applications, we have aimed to remove methylene blue (MB), methyl violet (MV), and toluidine blue O (TB), as model basic dyes, from aqueous solutions in the present study. Because their complex chemical structure makes them very stable to light, many chemicals, oxidizing agents and heat, the decolorization of dyes is very difficult by using conventional wastewater treatment techniques including coagulation, flocculation, biological oxidation, and chemical precipitation, etc.[3,6] On the other hand, the development of adsorption techniques provides a powerful alternative for the removal of dyes and also other pollutants from industrial wastewaters. In recent years, several materials and their activated carbon like clay,[7] tree leaves,[8] coconut coir,[9] titania,[10] surfactant-modified zeolite,[11] rice husk ash,[12] wheat straw,[13] etc. have been evaluated as adsorbents for the removal of dyes and other pollutants from wastewaters.

Agricultural and forestry products such as almond shell, maize cob waste, wood sawdust, and sunflower seed hull, etc. have great potential to be used as adsorbents since they contain polysaccharides and proteins having various functional groups such as carboxyl, hydroxyl and phosphates.[14] The almond shell (AS) is widely distributed in Turkey such that the annual production of AS is on average 30 000 tons in Turkey.[15] It was selected as an adsorbent for the removal of MB, MV, and TB dyes from aqueous solutions since it is found abundantly in nature and is cheap as compared to other adsorbents such as activated carbon or inorganic substances used in adsorption processes, and also it has no important industrial use.[16−18] The AS was used in this study without any physical or chemical pretreatment. Its utilization without any previous activation treatment is one of the significant features of this study with respect to a decrease in the cost of the adsorption process.

The main objectives of this paper were to (i) study the feasibility of using natural AS as an adsorbent in removal of MB, MV, and TB; (ii) evaluate the various experimental parameters affecting the adsorption process including initial pH of the aqueous solution, contact time, initial dye concentration, and temperature; (iii) evaluate the usefulness of various kinetic models (pseudofirst-order, pseudosecond-order, Elovich and intraparticle diffusion models); (iv) determine the applicability of isotherm models (Langmuir, Freundlich, Temkin, and Dubinin−Radushkevich); (v) decide the spontaneity and thermodynamic feasibility of the adsorption process with respect the thermodynamic parameters (Gibbs energy (ΔG), enthalpy (ΔH), and entropy (ΔS)).

2. MATERIALS AND METHODS

2.1. Preparation of Adsorbent. The AS (*P. dulcis*) was provided from a local market in Turkey and used without any

Received: November 10, 2010
Accepted: February 25, 2011
Published: March 16, 2011

dx.doi.org/10.1021/je101204j | *J. Chem. Eng. Data* 2011, 56, 2136–2147

Table 1. Physical and Chemical Properties of AS Used in the Experiments

parameters	
$S_{BET}/m^2 \cdot g^{-1}$	0.20
C	47.27
H	6.09
N	0.20
S	0.14
O[a]	46.10
ash content/%	0.20
water-soluble components[b]/%	0.80
moisture content/%	7.48
pH	5.40
pH_{PZC}	4.90
surface functional groups/mmol·g^{-1}	
carboxylic	0.90
phenolic	2.76
lactonic	1.14
total acidic value	4.80

[a] By difference. [b] Dry basis.

additional activation pretreatment except for washing and sieving to desired particle sizes. For preparation of AS for the adsorption experiments, it was washed with deionized water several times to remove surface impurities then dried for 4 days at 40 °C. The dried AS samples were ground in a blender and sieved to obtain a particle size of <150 μm and stored in glass containers. The surface functional groups of the natural AS were determined by utilizing Fourier transform infrared spectroscopy (FTIR) in our previous study.[16] Furthermore in the present study the FTIR spectra of the AS after adsorption and desorption of dye molecules were recorded between (400 and 4000) cm^{-1} in a Perkin-Elmer 1600 FTIR spectrometer in order to evaluate the changes in the band intensities. The specific surface area of AS was determined from the N_2 gas adsorption isotherm at 77 K using a Quantachrome Corporation, Autosorb-1-C/MS model specific surface area analyzer. Elemental analysis of AS was performed on a LECO CHNS 932 model apparatus. The surface acidic functional groups containing oxygen were determined according to a Boehm titration[19] and other characterization parameters were determined using standard methods[20] and are listed in Table 1.

2.2. Adsorbates. The basic dyes, MB (Figure 1a; CI: 52015; chemical formula: $C_{16}H_{18}ClN_3S$; molecular weight: 319.86 g·mol^{-1}, maximum wavelength: 662 nm), MV (Figure 1b; CI: 42535; chemical formula: $C_{25}H_{30}N_3Cl$; molecular weight: 393.96 g·mol^{-1}, maximum wavelength: 584 nm), and TB (Figure 1c; CI: 52040; chemical formula: $C_{15}H_{16}ClN_3S$; molecular weight: 305.83 g·mol^{-1}, maximum wavelength: 626 nm) were purchased from Sigma-Aldrich and were not purified prior to use. The stock dye solutions were prepared (5000 mg L^{-1}) in deionized water and the required concentration of working dye solutions were prepared by appropriate dilutions of the stock solutions.

2.3. Adsorption Experiments. For the adsorption experiments, the initial pH values of the dye solutions were adjusted to 8.0 by using either dilute HCl or NaOH solutions. The adsorption tests of the basic dyes onto AS were studied by using a batch process by mixing 100 mg of AS (10 g·L^{-1}) with 10 mL of dye solution over the concentration ranges of (100 to 1000) mg·L^{-1}, in polyethylene centrifuge tubes. The mixtures were agitated at a

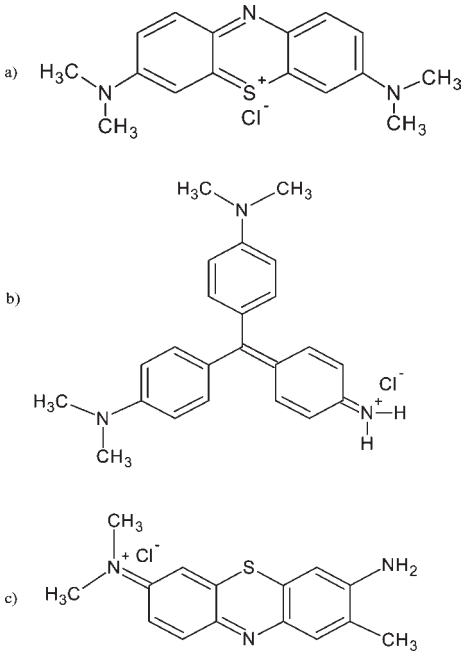

Figure 1. Chemical structure of (a) MB, (b) MV, and (c) TB.

speed of 400 rpm on a mechanical shaker (Edmund Bühler GmbH) for 30 min to reach equilibrium. After equilibrium, the adsorbent was separated from the dye solutions by filtration using 0.45 μm nitrocellulose membranes (Sartorius Stedim Biotech. GmbH) and the remaining concentration of dyes in the filtrate were determined by using a double beam UV−vis spectrophotometer (Unicam-UV 2) at wavelengths of 668 nm for MB, 586 nm for MV, and 630 nm for TB. All of the experiments were performed in triplicate to check the reproducibility of data and the averages of the results were used for data analysis. In the presented adsorption method, the relative standard deviation (RSD) was obtained after analysis a series of 20 replicates by contacting 10 mL of 100 mg·L^{-1} of dye solution with 10 g·L^{-1} of AS suspensions, individually, under the optimum experimental conditions. From the results, RSD values were found to be 6.5 % for MB, 5.0 % for MV, and 4.6 % for TB.

The concentration retained in the adsorbent phase (q_e, mg·g^{-1}) was calculated by using the following equation:

$$q_e = \frac{(C_o - C_e)V}{m_s} \quad (1)$$

C_o (mg·L^{-1}) is the initial dye concentration, C_e (mg·L^{-1}) is the equilibrium dye concentration in the aqueous solution, V (L) is the volume of solution, m_s (g) is the mass of the adsorbent, and q_e (mg·g^{-1}) is the calculated dye adsorption amount on AS.

3. RESULTS AND DISCUSSION

3.1. Effect of Initial pH. Previous research has shown that the adsorption of dye molecules onto an adsorbent is highly pH dependent since the functional groups, which are responsible for interaction between dye molecules and adsorbent, can be protonated or deprotonated to produce different surface charges in solution at different pH values.[21] Therefore the effects of initial solution pH were studied in the pH range of 2−10 for MB and TB and 3−10 for MV. The percentage removal increased from

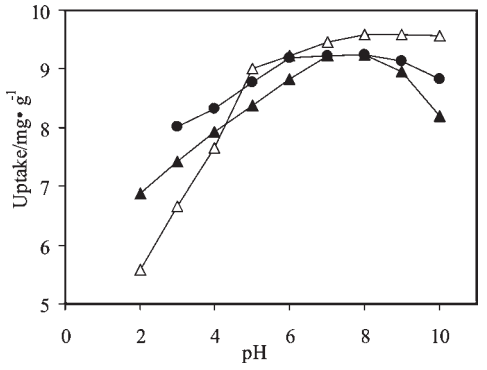

Figure 2. Effect of initial pH on dyes uptake by AS (initial MB, MV, and TB conc.: 100 mg·L^{-1}, AS conc.: 10 g·L^{-1}, contact time: 30 min, labeling: Δ, MB; ●, MV; ▲,TB).

56 % to 96 % for MB and 69 % to 92 % for TB when increasing the pH from 2 to 8 and from 80 % to 92 % for MV when increasing the pH from 3 to 8. The adsorption amount was approximately constant in the pH range of 8−10 for MB, whereas it decreased slowly after pH 8 for TB and MV (Figure 2).

The pH_{PZC} of any adsorbent is a very important characteristic that determines the pH at which the surface has net electrical neutrality. It is well-known that for basic dye adsorption, negatively charged groups on the adsorbent are necessary. At lower pH values ($pH < pH_{PZC}$) the surface charge of the surface of AS may get positively charged as a result of being surrounded by H_3O^+ ions and thus the competitive effects of H_3O^+ ions as well as the electrostatic repulsion between the dye molecules and the positively charged active adsorption sites on the surface of the AS lead to a decrease in the uptake of dye molecules. In contrast at higher pH values ($pH > pH_{PZC}$) the surface of AS may acquire a negative charge leading to an increase in dye uptake due to the electrostatic force of attraction. Because the pH_{PZC} value of AS was found to be 4.90, the cationic dyes can bind easily to the surface of AS, at a pH value higher than 4.90. On the other hand no valid reason can be given for the decrease in the adsorption amount of TB and MB after pH 8.0. Similar results were obtained for the adsorption of malachite green onto fresh water algae (*Pithophora* sp.).[22] As a result, the initial pH value was optimized as 8.0 for all three dyes.

3.2. Effect of Contact Time and Adsorption Kinetics. Figure 3a−c illustrates the effects of contact time on the removal of MB, MV, and TB, respectively, for different initial dye concentrations. The changes in contact time exhibit approximately the same effects on the three dyes. Because of the utilization of the readily available active adsorption sites on the AS surface, the adsorption of dyes was rapid for the first 15 min for all the investigated initial dye concentrations. Thereafter it continued at a slower rate and finally reached equilibrium as a result of saturation of AS surface sites. For all three dyes, at all of the studied initial dye concentrations a sufficient contact time was determined as 30 min.

The adsorption mechanism of MB, MV, and TB onto AS was evaluated by utilizing commonly used kinetic models including the pseudofirst-order, pseudosecond-order, Elovich, and intraparticle diffusion models.

The pseudofirst-order model is generally applicable over the initial stage of an adsorption process. The model has the following form:[23]

$$\frac{dq}{dt} = k_1(q_e - q_t) \qquad (2)$$

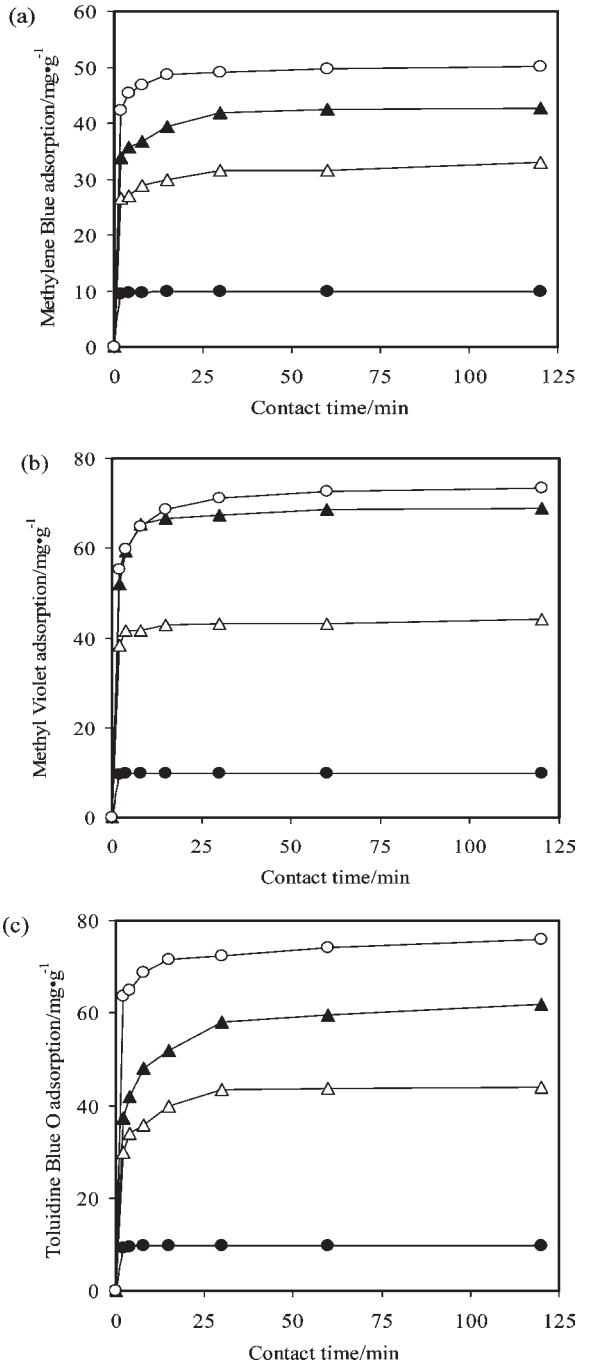

Figure 3. Effect of contact time on the adsorption of (a) MB, (b) MV, and (c) TB (initial pH: 8.0, AS conc.: 10 g·L^{-1}, labeling: ●, 100 mg L^{-1}; Δ, 450 mg L^{-1}; ▲, 750 mg L^{-1}; ○, 1000 mg L^{-1}).

where q_e (mg·g^{-1}) and q_t (mg·g^{-1}) are the amounts of the dyes adsorbed on the adsorbate at equilibrium and at any time t, respectively, and k_1 (min^{-1}) is the rate constant of the first order adsorption. After integration and applying boundary conditions $q_t = 0$ at $t = 0$ and $q_t = q_t$ at $t = t$ the integrated form of eq 2 becomes

$$\ln(q_e - q_t) = \ln q_e - k_1 t \qquad (3)$$

A straight line of $\ln(q_e - q_t)$ versus t suggests the applicability of this kinetic model and q_e and k_1 can be determined from the intercept and slope of the plot, respectively.

The pseudosecond-order model assumes that the rate limiting step is chemical sorption or chemisorption and predicts the behavior over the whole range of adsorption. The model is in the following form:[24]

$$\frac{dq}{dt} = k_2(q_e - q_t)^2 \quad (4)$$

where k_2 ($g \cdot mg^{-1} \cdot min^{-1}$) is the rate constant of the second-order equation, q_e ($mg \cdot g^{-1}$) is the maximum adsorption capacity, and q_t ($mg \cdot g^{-1}$) is the amount of adsorption at time t (min). After definite integration by applying the conditions $q_t = 0$ at $t = 0$ and $q_t = q_t$ at $t = t$, eq 4 becomes the following:

$$\frac{t}{q_t} = \frac{1}{k_2 q_e^2} + \frac{t}{q_e} \quad (5)$$

If second-order kinetics is applicable, a plot of t/q_t against t gives a straight line and q_e and k_2 can be obtained from the slope and intercept of the plot, respectively.

The Elovich model is useful for energetically heterogeneous solid surfaces and is given in the following equation:[25]

$$q_t = 1/\beta \ln(\alpha\beta) + 1/\beta \ln t \quad (6)$$

where α ($mg \cdot g^{-1} \cdot min^{-1}$) is the initial sorption rate and β ($g \cdot mg^{-1}$) is related to the extent of surface coverage and the activation energy for chemisorption. If MB, MV, and TB adsorption onto AS fits the Elovich model, plots of q_t versus $\ln(t)$ should give a linear relationship with a slope of $(1/\beta)$ and an intercept of $(1/\beta) \ln(\alpha\beta)$.

The kinetic constants were obtained from the slope and intercept of the plots of $\ln(q_e - q_t)$ versus t (pseudofirst order), t/q_t against t (pseudosecond order), and q_t versus $\ln(t)$ (Elovich model) and are given in Table 2. For the pseudofirst order model, the obtained R^2 values were relatively low and the calculated q_e values ($q_{e,cal}$) were much lower than the experimental values of q_e ($q_{e,exp}$).Also the small R^2 values obtained from the Elovich model suggested that it was not appropriate to use for the prediction of the kinetics of MB, MV and TB adsorption onto AS. On the other hand the pseudosecond order model had $q_{e,cal}$ values that agreed very well with the $q_{e,exp}$ values and the R^2 values were closer to unity for all three dyes at different initial concentrations. Hence the pseudo-second order model is suitable for describing the adsorption kinetics of MB (Figure 4a), MV (Figure 4b), and TB (Figure 4c) onto AS. This suggests that the present adsorption process is a chemisorption process involving exchange or sharing of electrons between the dye cations and functional groups of AS.[26]

The intraparticle diffusion model equation is expressed as[27]

$$q_t = k_{id} t^{1/2} + c \quad (7)$$

where q_t ($mg \cdot g^{-1}$) is the amount of sorption at time t (min) and k_{id} ($mg \cdot g^{-1} \cdot min^{-1/2}$) is the rate constant of the intraparticle diffusion model. The magnitude of C gives an idea about the thickness of the boundary layer such that high values show a large effect of the boudary layer. The plot of q_t versus $t^{1/2}$ may present multilinearity indicating that any adsorption process takes place in three main steps. The first portion is attributed to the transport of adsorbate molecules from the bulk solution to the adsorbent external surface by diffusion through the boundary layer (film diffusion). The second portion describes the diffusion of the adsorbate from the external surface into the pores of the adsorbent (pore or intraparticle diffusion). The last step is relevant to the adsorption of the adsorbate on the active sites on the internal surface of the pores. The last step generally occurs rapidly thus the overall adsorption should be controlled by either film or pore diffusion, or a combination of both. If plots of q_t versus $t^{1/2}$ pass through the origin, pore diffusion is the only rate limiting step; if not it is considered that the adsorption process is also controlled by film diffusion in some cases.[28,29]

By evaluating the intraparticle mass transfer curve of the three dyes for different initial dye concentrations, it was observed that the MB, MV and TB adsorption processes were found to follow two distinct phases which were film diffusion (first stage) and intraparticle diffusion (second step). The intraparticle rate constants for the first phase ($k_{id,1}$) and second phase ($k_{id,2}$) and c parameters were obtained from the plot of q_t versus $t^{1/2}$ and the results are given in Table 2. For all three dyes, by comparing the rate constants, the lower values of $k_{id,2}$ than $k_{id,1}$ indicating that the rate limiting step is intraparticle diffusion. The C values, obtained from the intercept of the q_t versus $t^{1/2}$ plots, indicate that the line did not pass through the origin hence intraparticle diffusion is not the only rate limiting mechanism. In the light of these results, it can be concluded that the adsorption of MB, MV, and TB onto AS is a complex process and both intraparticle diffusion and surface sorption contributes to the rate-limiting step.

3.3. Effect of Initial Adsorbate Concentration and Adsorption Isotherms. The effects of initial dye concentration on the adsorption process were evaluated by varying the initial dye concentrations in the range of (100 to 1000) $mg \cdot L^{-1}$ (Figure 5a−c). The amount of adsorbed dye cations per unit mass of the AS increased with increasing initial dye concentrations. This is because the initial dye concentration acts as a driving force to overcome mass transfer resistance for dye transport between the aqueous solution and the surface of the AS. Also the increase in initial dye concentration enhances the interaction between the AS and dye cations. However, as a result of saturation of the active adsorption sites on the AS surface at higher dye concentrations, the adsorption percentages decreased for all three dye cations.[30]

Adsorption isotherm models provide useful data in order to understand the mechanisms of the adsorption process, to describe how an adsorbate interacts with an adsorbate and to evaluate the applicability of the process. The Langmuir, Freundlich, Temkin, and Dubinin−Radushkevich isotherm models were used to describe the relationship between the amount of dye cations adsorbed onto the AS and their equilibrium concentrations in aqueous solution.

The Langmuir isotherm model predicts the existence of monolayer coverage of the sorbates such that when an adsorption site on the adsorbent surface is occupied by a sorbate, no further sorption can take place at this site. The model is based on the assumption that adsorption takes place at specific homogeneous sites within the adsorbent and there is no interaction between the adsorbed species. The model has the following form:[31]

$$q_e = \frac{bq_{max}C_e}{1 + bC_e} \quad (8)$$

where q_e ($mg \cdot g^{-1}$) is the amount of the dye cations adsorbed per unit mass of adsorbent, C_e ($mg \cdot L^{-1}$) is the equilibrium dye concentration in aqueous solution, and q_{max} ($mg \cdot g^{-1}$) and b ($L \cdot mg^{-1}$) are the Langmuir constants related to the adsorption capacity and free energy or net enthalpy of adsorption, respectively. The Langmuir model in linear form is

$$\frac{C_e}{q_e} = \frac{C_e}{q_{max}} + \frac{1}{bq_{max}} \quad (9)$$

Table 2. Kinetic Model Parameters for Adsorption of MB, MV, and TB on AS

MB							
		pseudofirst-order			pseudosecond-order		
C_o/mg·L^{-1}	$q_{e,exp}$/mg·g^{-1}	k_1/min^{-1}	$q_{e,cal}$/mg·g^{-1}	R^2	k_2/g·mg^{-1}·min^{-1}	$q_{e,cal}$/mg·g^{-1}	R^2
100	9.95	−0.072	0.74	0.6027	0.500	10.00	0.9999
450	33.06	−0.038	8.54	0.5801	0.023	33.22	0.9996
750	42.75	−0.071	13.05	0.8706	0.023	43.10	0.9999
1000	50.20	−0.054	8.73	0.6209	0.035	50.25	0.9999

	intraparticle diffusion model					Elovich model		
Co/mg·L^{-1}	$k_{id,1}$/mg·g^{-1}·min$^{-1/2}$	R^2	$k_{id,2}$/mg·g^{-1}·min$^{-1/2}$	R^2	C	β/g·mg^{-1}	α/mg·g^{-1}·min^{-1}	R^2
100	0.118	0.8998	0.007	0.9903	9.60	0.104	5.22×10^{39}	0.9194
450	1.516	0.9625	0.288	0.8634	26.52	1.664	3.86×10^{6}	0.9697
750	2.147	0.9714	0.169	0.8855	34.40	2.378	8.45×10^{5}	0.9508
1000	2.423	0.9236	0.217	0.9903	44.20	1.786	2.24×10^{10}	0.8839

MV							
		pseudofirst-order			pseudosecond-order		
C_o/mg·L^{-1}	$q_{e,exp}$/mg·g^{-1}	k_1/min^{-1}	$q_{e,cal}$/mg·g^{-1}	R^2	k_2/g·mg^{-1}·min^{-1}	$q_{e,cal}$/mg·g^{-1}	R^2
100	9.96	−0.068	0.54	0.5131	0.940	9.97	0.9999
450	44.18	−0.040	5.93	0.4069	0.042	44.25	0.9999
750	68.78	−0.093	17.91	0.8775	0.024	68.96	0.9999
1000	73.38	−0.065	21.82	0.8372	0.013	74.07	0.9999

	intraparticle diffusion model					Elovich model		
C_o/mg·L^{-1}	$k_{id,1}$/mg·g^{-1}·min$^{-1/2}$	R^2	$k_{id,2}$/mg·g^{-1}·min$^{-1/2}$	R^2	C	β/g·mg^{-1}	α/mg·g^{-1}·min^{-1}	R^2
100	0.102	0.9745	0.007	0.9903	9.71	0.076	1.23×10^{55}	0.8965
450	1.553	0.7663	0.183	0.7498	40.00	1.162	3.63×10^{14}	0.8161
750	5.86	0.8551	0.242	0.7072	57.50	3.757	1.63×10^{6}	0.7785
1000	5.365	0.9717	0.379	0.9032	58.14	4.542	1.50×10^{5}	0.9316

TB							
		pseudofirst-order			pseudosecond-order		
C_o/mg·L^{-1}	$q_{e,exp}$/mg·g^{-1}	k_1/min^{-1}	$q_{e,cal}$/mg·g^{-1}	R^2	k_2/g·mg^{-1}·min^{-1}	$q_{e,cal}$/mg·g^{-1}	R^2
100	9.81	−0.042	0.74	0.3420	0.378	9.81	0.9999
450	43.89	−0.084	16.71	0.8659	0.017	44.44	0.9999
750	61.90	−0.047	26.87	0.8226	0.007	62.89	0.9997
1000	75.85	−0.044	16.65	0.6240	0.014	76.33	0.9999

	intraparticle diffusion model					Elovich model		
C_o/mg·L^{-1}	$k_{id,1}$/mg·g^{-1}·min$^{-1/2}$	R^2	$k_{id,2}$/mg·g^{-1}·min$^{-1/2}$	R^2	C	β/g·mg^{-1}	α/mg·g^{-1}·min^{-1}	R^2
100	0.121	0.6881	0.031	0.9999	9.41	0.101	1.28×10^{40}	0.8408
450	3.718	0.9629	0.072	0.9992	31.92	3.610	2.90×10^{3}	0.9224
750	6.013	0.9715	0.714	0.9989	39.26	6.251	2.40×10^{2}	0.9706
1000	3.322	0.9869	0.629	0.9856	64.27	3.061	5.92×10^{8}	0.9679

The Langmuir model constants, q_{max} and b, can be calculated from the slope and intercept of the linear plot of C_e/q_e versus C_e, respectively.

The essential characteristics of the Langmuir isotherm can be expressed by means of "R_L" a dimensionless constant, called the separation factor or equilibrium parameter. R_L can be calculated using the following equation:[32]

$$R_L = \frac{1}{1 + bC_o} \tag{10}$$

dx.doi.org/10.1021/je101204j |J. Chem. Eng. Data 2011, 56, 2136–2147

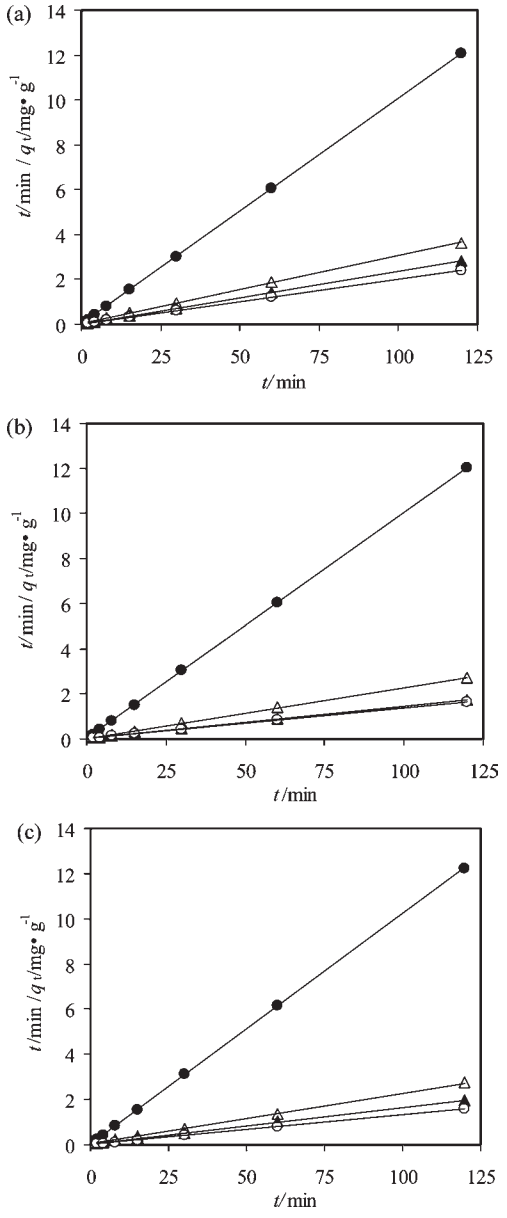

Figure 4. Pseudosecond order kinetic model for (a) MB, (b) MV, and (c) TB (labeling: ●, 100 mg L^{-1}; Δ, 450 mg L^{-1}; ▲, 750 mg L^{-1}; ○, 1000 mg L^{-1}).

where C_o ($mg \cdot L^{-1}$) is the initial concentration of sorbate and b ($L \cdot mg^{-1}$) is the Langmuir constant described above. There are four possibilities for the R_L value:

- for favorable sorption $0 < R_L < 1$
- for unfavorable sorption $R_L > 1$
- for linear sorption $R_L = 1$
- for irreversible sorption $R_L = 0$

The Freundlich isotherm model assumes that the adsorption takes place on heterogeneous surfaces which have different adsorption energies. The model has the following form:[33]

$$q_e = K_f C_e^{1/n} \quad (11)$$

where K_f is a constant related to sorption capacity ($mg \cdot g^{-1}$) and $1/n$ is an empirical parameter related to sorption intensity.

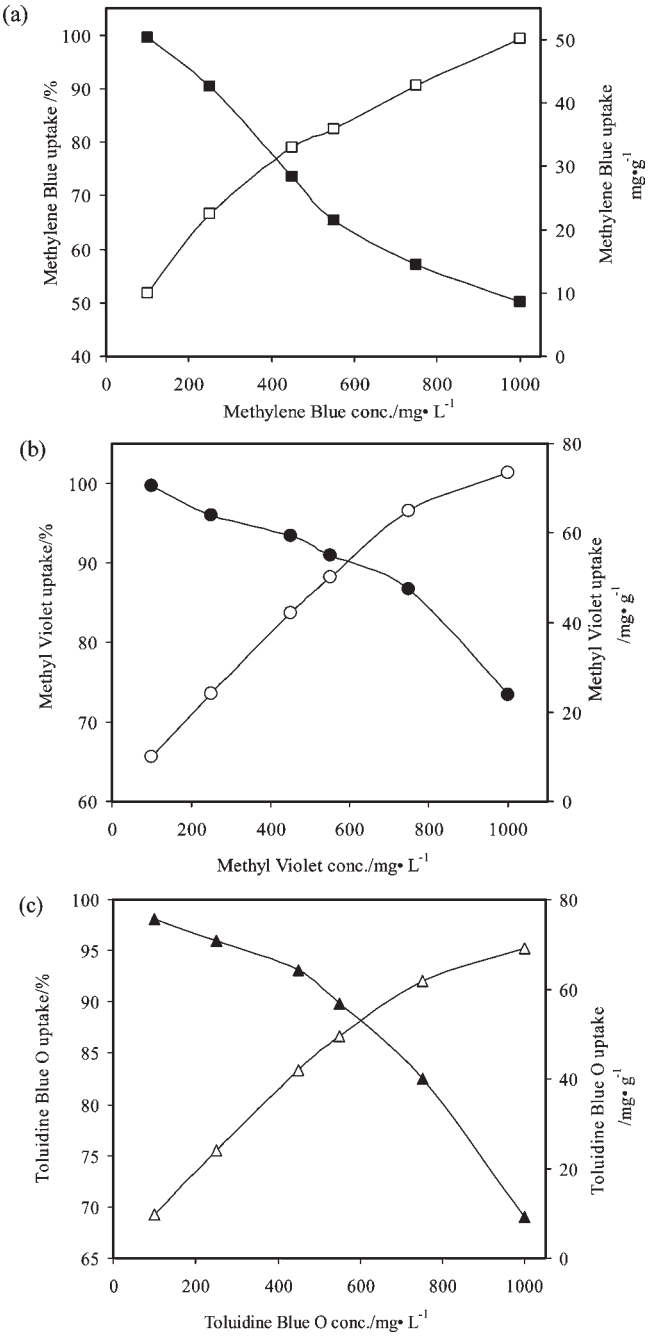

Figure 5. (a) Effect of initial MB concentration (AS conc.: 10 $g \cdot L^{-1}$, labeling: ■, MB uptake/%; □, MB uptake/$mg \cdot g^{-1}$. (b) Effect of initial MV concentration (AS conc.: 10 $g \cdot L^{-1}$, labeling: ●, MV uptake/ %; ○, MV uptake/$mg \cdot g^{-1}$. (c) Effect of initial TB concentration (AS conc.: 10 $g \cdot L^{-1}$, labeling: ▲, TB uptake/ %; Δ, TB uptake/$mg \cdot g^{-1}$).

The Freundlich model in linear form is

$$\ln q_e = \ln K_f + \frac{1}{n} \ln C_e \quad (12)$$

The Freundlich constants, K_f and $1/n$, can be determined from the intercept and slope of linear plot of ln q_e versus ln C_e, respectively.

The Temkin isotherm model assumes that the heat of adsorption of all molecules decreases linearly with coverage

dx.doi.org/10.1021/je101204j |J. Chem. Eng. Data 2011, 56, 2136–2147

due to adsorbate/adsorbate interactions. The Temkin isotherm is given as[34]

$$q_e = \mathrm{RT}/b(\ln AC_e) \quad (13)$$

$$B = RT/b \quad (14)$$

where B ($J \cdot mol^{-1}$) is the Temkin constant related to heat of adsorption, A ($L \cdot g^{-1}$) is the equilibrium binding constant corresponding to the maximum binding energy, R (8.314 $J \cdot mol^{-1} \cdot K^{-1}$) is the universal gas constant, and T (Kelvin) is the absolute solution temperature.

The Temkin model in linear form is

$$q_e = B(\ln A) + B(\ln C_e) \quad (15)$$

The Temkin constants, A and B, can be determined from the intercept and slope of linear plot of q_e versus ln C_e, respectively.

The Dubinin−Radushkevich (D-R) isotherm model gives an idea about the type of the adsorption. The model is given as follows:[35]

$$q_e = q_m \exp(-\beta\varepsilon^2) \quad (16)$$

where q_e ($mol \cdot g^{-1}$) is the amount of dye adsorbed per unit mass of adsorbent, q_m ($mol \cdot g^{-1}$) is the monolayer adsorption capacity, β ($mol^2 \cdot kJ^{-2}$) is the activity coefficient related to the mean sorption energy, and ε is the Polanyi potential and can be calculated by the following equation:

$$\varepsilon = RT \ln(1 + 1/C_e) \quad (17)$$

where C_e ($mol \cdot L^{-1}$) is the equilibrium dye concentration in aqueous solution. The mean adsorption energy, E ($kJ \cdot mol^{-1}$), gives information about the mechanisms of the adsorption process. If E value lies between (8 and 16) $kJ \cdot mol^{-1}$ the adsorption process takes place chemically, whereas when E < 8 kJ mol^{-1}, the adsorption process proceeds physically.[36] The E value can be calculated using the following equation:

$$E = 1/(-2\beta)^{1/2} \quad (18)$$

The linear form of D-R isotherm model is expressed as

$$\ln q_e = \ln q_m - \beta\varepsilon^2 \quad (19)$$

The D-R model constants, q_m and β, can be determined from the intercept and slope of linear plot of ln q_e versus ε^2, respectively.

The experimental equilibrium data of MB (Figure 6a), MV (Figure 6b), and TB (Figure 6c) were compared with the theoretical equilibrium data obtained from the Langmuir, Freundlich, Temkin, and Dubinin−Radushkevich isotherm models. The isotherm constants were calculated by evaluating the linearized form of the models (figures not shown). All of the isotherm constants and correlation coefficients are given in Table 3. The adsorption capacity of AS was found to be 51.02 $mg \cdot g^{-1}$ for MB, 76.34 $mg \cdot g^{-1}$ for MV, and 72.99 $mg \cdot g^{-1}$ for TB by using the Langmuir model equation. The adsorption capacity of AS was compared with the adsorption capacities of other adsorbents in the literature,[6,24,37−44] and the comparative data are given in Table 4. In most cases the adsorption capacity of AS was found to be better than the other adsorbents reported in the literature. The R_L values ranged from 0.28 to 0.04 for MB, from 0.18 to 0.02 for MV, and from 0.17 to 0.02 for TB, between (100 and 1000) mg L^{-1} of initial dye concentration, indicating that the MB, MV, and TB adsorption onto AS is favorable under the studied conditions. In addition, the low R_L values implied that the interaction of dye molecules with AS might be relatively strong.[45] The Freundlich isotherm constant, n, gives an idea for the favorability of the adsorption process. The value of n should be less than 10 and higher than unity for favorable adsorption conditions. As can be seen from Table 3, the n values for MB, MV, and TB were in the range of 1−10, indicating that the adsorption is a favorable process. By evaluating the D-R isotherm model, the mean adsorption energy, E, values were found to be 16.67 $kJ \cdot mol^{-1}$ for MB, 14.43 $kJ \cdot mol^{-1}$ for MV, and 12.13 $kJ \cdot mol^{-1}$ for TB, suggesting that the adsorption mechanisms of MB, MV, and TB onto AS is

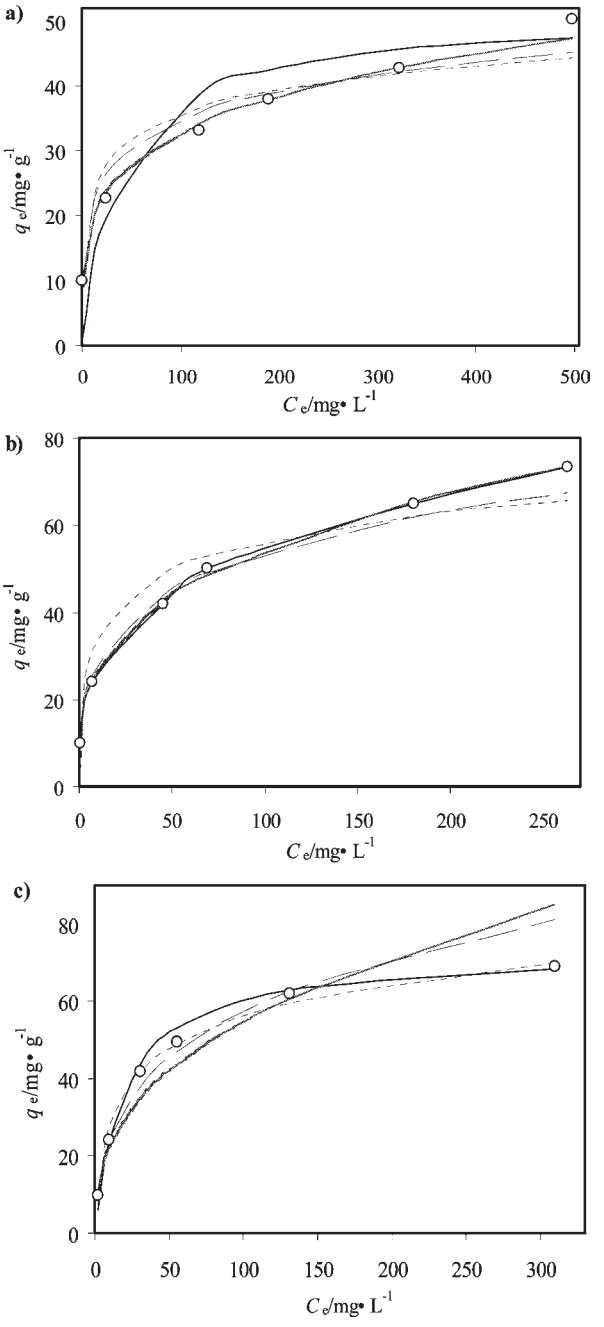

Figure 6. Comparison of equilibrium isotherms between the experimental data and theoretical data for (a) MB uptake, (b) MV uptake, and (c) TB uptake (labeling: ○, experimental; —, Langmuir; ···, Freundlich; ---, Temkin; − −, Dubinin−Radushkevich).

Table 3. Langmuir, Freundlich, Temkin, and Dubinin Radushkevich (D-R) Isotherm Parameters for the Adsorption of MB, MV, and TB on AS

	type of dye		
	MB	MV	TB
Langmuir isotherm model			
q_{max}/mg·g^{-1}	51.02	76.34	72.99
b/L·mg^{-1}	0.026	0.045	0.048
R^2	0.9769	0.9815	0.9981
Freundlich isotherm model			
K_f/mg·g^{-1}	11.36	13.17	9.08
n	4.34	3.24	2.56
R^2	0.9961	0.9996	0.9515
Temkin isotherm model			
A/L·g^{-1}	7.03	3.66	0.98
B	5.43	9.56	12.23
b/J·mol^{-1}	456.30	259.16	202.58
R^2	0.9185	0.9259	0.9891
D-R isotherm model			
q_m/mg·g^{-1}	71.53	148.09	211.15
β/kJ^2·mol^{-2}	0.0018	0.0024	0.0034
E/kJ·mol^{-1}	16.67	14.43	12.13
R^2	0.9777	0.9916	0.9810

chemical in nature. By comparing the correlation coefficient values obtained from the Langmuir and Freundlich isotherm models, it can be concluded that the Langmuir isotherm model is more suitable for TB while the experimental data obtained for MB and MV adsorption were fitted well by the Freundlich isotherm model. This may be due to both homogeneous and heterogeneous distribution of active sites on the surface of the AS.

3.4. Effect of Temperature and Thermodynamics of Adsorption. The adsorption experiments were carried out at (5, 15, 25, and 40) °C in order to investigate the effects of temperature on the adsorption of MB, MV, and TB onto AS. A slight increase was obtained in the adsorption amount of all three dyes with increasing temperature. The adsorption efficiency increased from 9.5 mg·g^{-1} (95.0 % removal) to 9.9 mg·g^{-1} (99.0 % removal) for MB, from 13.4 mg·g^{-1} (89.3 % removal) to 14.6 mg·g^{-1} (97.3 % removal) for MV, and from 18.5 mg·g^{-1} (92.5 % removal) to 19.7 mg·g^{-1} (98.5 % removal) for TB, when the temperature was increased from (5 to 40) °C. Figure 7a indicates that the adsorption process of dye cations was endothermic in nature. It is well-known that the diffusion rate of the adsorbate molecules across the external boundary layer and in the internal pores of adsorbent particles increases and viscosity of the aqueous solution decreases by increasing the temperature of the adsorption medium.[21] On the other hand, previous research based on the adsorption of methylene blue by invasive marine seaweed, showed that the adsorption amount of MB was not affected by increasing the temperature.[46]

The thermodynamic parameters including Gibbs energy (ΔG), enthalpy (ΔH), and entropy (ΔS) have a significant role in determining the feasibility, spontaneity, and heat change of the adsorption process. These parameters can be calculated using the following equations:[47]

$$\Delta G = -RT \ln K_d \quad (20)$$

where R is the universal gas constant (8.314 J·mol^{-1}·K^{-1}), T is the temperature (K), and K_d is the distribution coefficient.

Table 4. Comparison of Adsorption Capacities of Different Adsorbents Reported in the Literature

	adsorption capacities/mg·g^{-1}			
adsorbent	MB	MV	TB	ref
mansonia wood sawdust		17.7		6
granular activated carbon		95.0		37
bagasse fly ash		26.2		38
Posidonia oceanica (L.) fibres	5.6			26
rice husk	40.6			39
neem leaf powder	8.8			40
coir pith activated carbon	5.9			41
carbon nanotubes	35.4−64.7			42
gypsum			28.0	43
Turkish zeolite			64.2	44
almond shell	51.0	76.3	73.0	this work

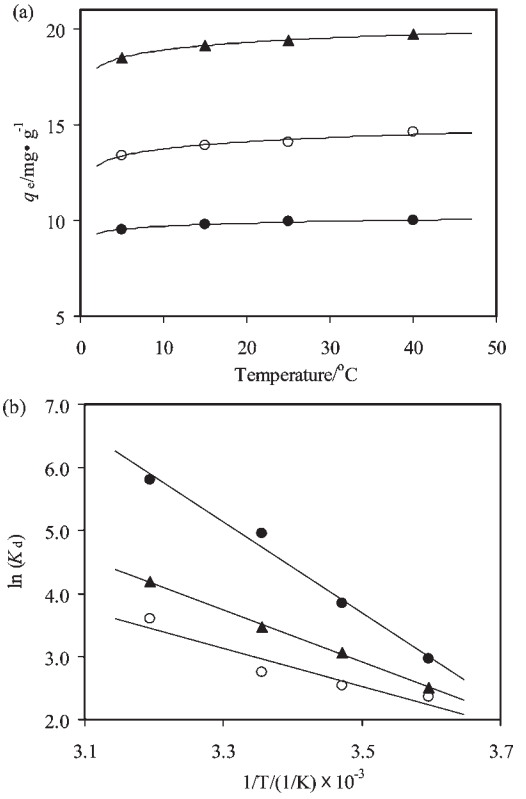

Figure 7. (a) Effect of temperature on dyes uptake (initial pH: 8.0, initial MB conc.: 100 mg·L^{-1}, initial MV conc.: 150 mg·L^{-1}, initial TB conc.: 200 mg·L^{-1}, AS conc.: 10 g·L^{-1}, contact time: 30 min, labeling: ▲, TB; ○, MV; ●, MB). (b) The plot between ln K_d versus $1/T$ for obtaining the thermodynamic parameters (labeling: ▲, TB; ○, MV; ●, MB).

The K_d value was calculated using the following equation:

$$K_d = q_e/C_e \quad (21)$$

where q_e (mg·L^{-1}) and C_e (mg·L^{-1}) are the equilibrium concentration of dye cations adsorbed onto AS and remained in the solution, respectively. The enthalpy (ΔH) and entropy change (ΔS) of adsorption were estimated from the

dx.doi.org/10.1021/je101204j |J. Chem. Eng. Data 2011, 56, 2136–2147

Table 5. Thermodynamic Parameters of MB, MV, and TB Adsorption on AS at Different Temperatures

	thermodynamic constants				
	T/°C	K_d	ΔG/kJ·mol^{-1}	ΔS/(J·mol^{-1}·K^{-1})[a]	ΔH/(kJ·mol^{-1})[a]
MB	5	19.41	− 6.85	241.0	60.0
	15	46.62	− 9.20		
	25	141.86	−12.28		
	40	332.33	− 15.11		
MV	5	10.59	− 5.46	109.37	25.26
	15	12.64	− 6.07		
	25	15.67	− 6.82		
	40	36.50	− 9.36		
TB	5	12.33	− 5.81	144.05	34.23
	15	21.22	− 7.32		
	25	32.33	− 8.61		
	40	65.67	−10.89		

[a] Measured between 278 and 313 K.

following equation:

$$\Delta G = \Delta H - T\Delta S \quad (22)$$

This equation can be written as

$$\ln K_d = \frac{\Delta S}{R} - \frac{\Delta H}{RT} \quad (23)$$

ΔH and ΔS were calculated from the slope and intercept of the van't Hoff plot of ln K_d versus $1/T$, respectively (Figure 7b). The thermodynamic parameters for the adsorption of MB, MV, and TB onto AS are given in Table 5. The negative values of ΔG, in the temperature range of (5 to 40) °C, for all three dyes, suggest the feasibility of the process and spontaneous nature of the adsorption of MB, MV, and TB onto AS while the positive value of ΔH indicated the endothermic nature of the adsorption which was also supported by the increase in amount of dye uptake of the adsorbent with a rise in temperature. The positive value of ΔS reflected the good affinity of MB, MV, and TB toward the AS and the increased randomness at the solid/solution interface during the adsorption of MB, MV, and TB onto AS.

3.5. Desorption and Reusability without Regeneration. Desorption of the adsorbed dye cations from AS was studied in a batch system. First step, 10 g·L^{-1} of AS suspensions was equilibrated with 10 mL of 100 mg·L^{-1} initial dye solutions at pH 8.0, individually. After reaching equilibrium the AS was separated by filtration then the equilibrium concentrations of the dyes in the filtrates were determined by UV−vis spectrophotometer. Secondary step; after washing the dye loaded AS with deionized water several times to remove the surface residual dye cations, it was treated with 10 mL of different types of desorption solutions by agitating at 400 rpm for 30 min. For MB and TB, 0.5 M HCl in 60 % (v/v) methanol was selected as the best desorption solution, while for MV, 1 M NaCl in 60 % (v/v) methanol exhibited the best desorption efficiency (Table 6). By comparing the FTIR spectrum obtained after adsorption of MB, MV and TB onto AS (Figure 8a) and after desorption of dye molecules (Figure 8b), it is important to notice that the band intensities increased after desorption of the dye molecules.

The adsorption experiments were performed to test the reusability of MB, MV and TB loaded AS without regeneration by contacting dye solutions (initial concentrations of 100 mg·L^{-1}) with 10 g·L^{-1} of AS suspensions, individually. After shaking for 30 min, the dye loaded AS was separated and then treated with another 100 mg·L^{-1} of dye solution. The process was repeated five times. The largest adsorption amount of MB (96.7 % removal), MV (98.5 % removal), and TB (96.8 % removal) was obtained with fresh AS (first cycle), and in each of their subsequent loading the adsorption capacity of AS decreased. After cycle 5, the adsorption amount of MB was 2.10 mg·g^{-1} (21.0 % removal), MV was 1.29 mg·g^{-1} (12.9 % removal), and TB was 4.33 mg·g^{-1} (43.3 % removal). The results suggested that already used AS can be applied for MB, MV, and TB adsorption at least five times without regeneration.

Table 6. Desorption Efficiencies of Different Types of Desorption Solutions

	desorption efficiencies/%		
types of desorption solutions	MB	MV	TB
methanol (50 %, v/v)	7.5 ± 1.5	11.0 ± 0.8	5.7 ± 1.2
acetone (50 %, v/v)	37.8 ± 0.9	49.4 ± 4.1	23.6 ± 2.9
1 M NaCl	13.0 ± 0.2	5.8 ± 1.0	5.1 ± 0.5
1 M acetic acid	60.1 ± 2.0	26.9 ± 0.8	45.9 ± 3.7
1 M NaCl in methanol (60 %, v/v)	78.0 ± 1.7	81.0 ± 3.6	69.8 ± 1.8
0.5 M HNO_3	11.0 ± 0.6	2.0 ± 0.1	3.2 ± 0.2
0.5 M HNO_3 in methanol (60 %, v/v)	80.2 ± 4.4	8.0 ± 0.1	69.1 ± 1.8
1 M HNO_3	18.1 ± 2.5	2.5 ± 0.7	7.1 ± 1.9
0.5 M HCl	28.7 ± 1.9	6.9 ± 0.1	14.1 ± 0.3
0.5 M HCl in methanol (60 %, v/v)	81.4 ± 3.1	10.1 ± 0.5	82.2 ± 0.9

Table 7. Removal of MB, MV, and TB in Stream and Sea Water[a]

		stream water			sea water		
	added/μg	C_e/μg	q_e/μg	% removal	C_e/μg	q_e/μg	% removal
MB	0	ND			ND		
	250	6.4 ± 1.1	243.6	97.4	17.9 ± 1.3	232.1	92.8
	500	12.0 ± 0.1	488.0	97.6	43.6 ± 1.2	456.4	91.3
MV	0	ND			ND		
	250	12.7 ± 0.5	237.2	94.9	14.3 ± 0.3	235.7	94.3
	500	19.4 ± 1.3	480.6	96.1	22.3 ± 0.6	477.7	95.5
TB	0	ND			ND		
	250	15.9 ± 0.3	234.1	93.6	18.4 ± 1.9	231.6	92.6
	500	22.6 ± 0.8	477.4	95.5	34.8 ± 1.1	465.2	93.0

[a] Initial pH: 8.0, sample volume: 25 mL, AS concentration: 10 g·L^{-1}.

3.6. Application to Real Samples. In order to evaluate the applicability of the present removal process based on the adsorption of MB, MV, and TB onto AS, the procedure was applied to a stream (Degirmendere, Trabzon/Turkey) and seawater (Black Sea, Trabzon/Turkey) as real liquid samples. For that purpose the water samples were filtered through a cellulose membrane of pore size 0.45 μm and collected in prewashed (in turn with detergent, doubly distilled/deionized water, dilute HNO_3, and doubly distilled/deionized water) polyethylene bottles. The water samples were collected daily. Prior to dye analysis the pH of the samples was adjusted to 8.0 and the proposed procedure given in section 2.3 was applied to the samples. Different amounts of dye

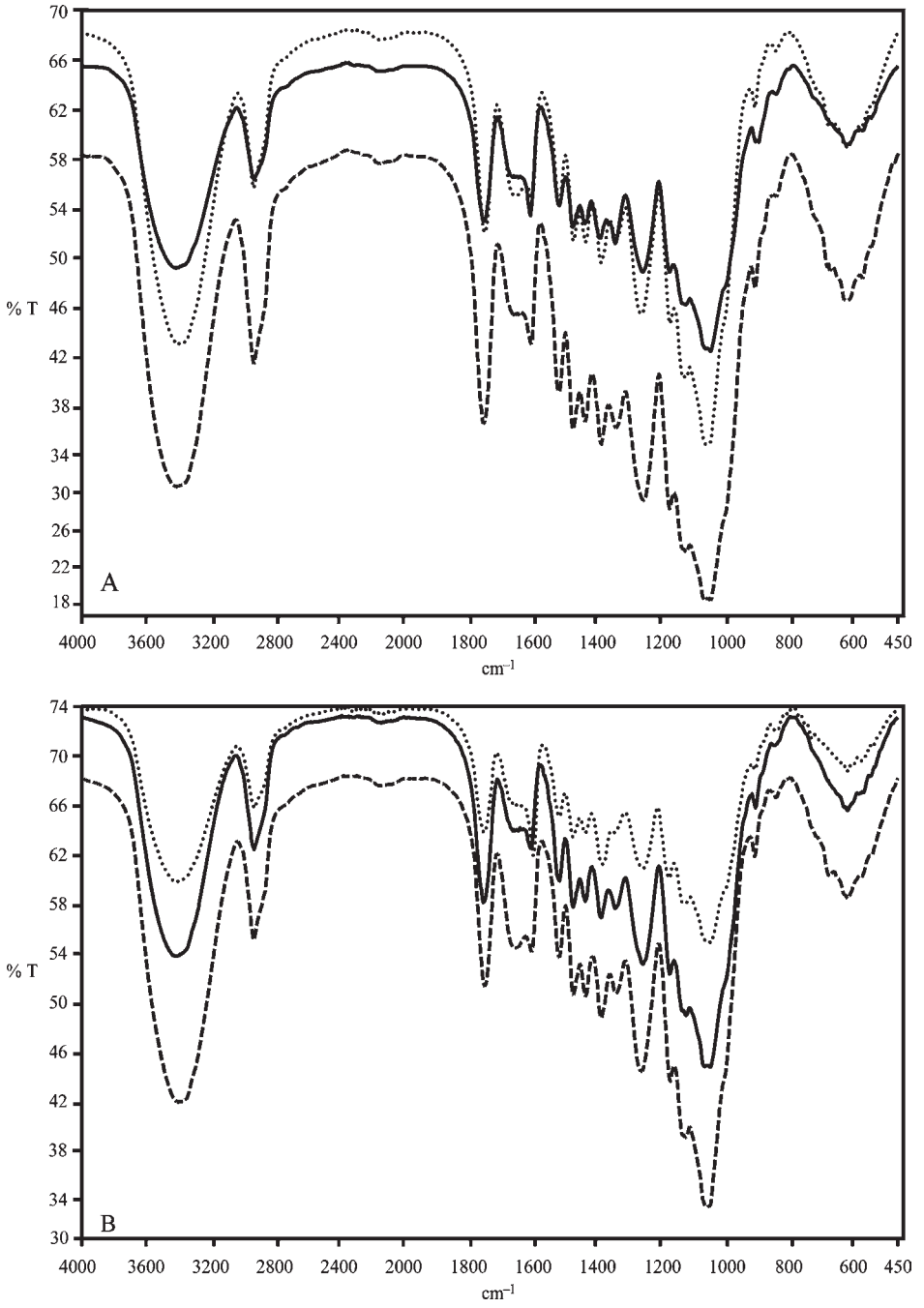

Figure 8. (a) FTIR spectra of MB, MV, and TB loaded AS. (b) FTIR spectra of AS after desorption (labeling: ···, MV; ---, TB; —, MB).

species were also spiked into these samples and good removal efficiencies were obtained for all three dyes (Table 7).

4. CONCLUSIONS

The adsorption processes require use of adsorbents which are low cost, easily available, and possess high pollutant uptake capacity. Hence we have aimed to assess the potential utilization of AS, which is an agricultural byproduct, in removal of highly toxic and water-soluble basic dyes, MB, MV and TB from aqueous solutions. The present study offers two major advantages (i) The AS is an agricultural waste material so this waste represents unused resources and also presents serious disposal problems. (ii) The AS was used without any previous activation treatment which decreases the adsorption costs.

The adsorption characteristics of MB, MV, and TB onto AS were evaluated in terms of equilibrium, kinetic, and thermodynamic parameters. The adsorption kinetics was predicted by the pseudosecond order model. As a result of the thermodynamic evaluation of MB, MV, and TB adsorption, the obtained negative ΔG values revealed that the adsorption of MB, MV, and TB onto AS was thermodynamically feasible and spontaneous, the positive values of ΔH suggested the endothermic nature of adsorption, and the positive values of ΔS indicated the increasing randomness at the solid/solution interface during the adsorption process.

On the basis of all results, it can be concluded that natural AS can be used effectively in removal of MB, MV, and TB from aqueous solutions using the described adsorption process.

AUTHOR INFORMATION

Corresponding Author

*Tel: +90 462 3774241. Fax: +90 462 3253196. E-mail: cduran@ktu.edu.tr.

REFERENCES

(1) Chen, S.; Zhang, J.; Zhang, C.; Yue, Q.; Li, Y.; Li, C. Equilibrium and kinetic studies of methyl orange and methyl violet adsorption on activated carbon derived from *Phragmites australis*. *Desalination* **2010**, *252*, 149–156.

(2) Hamdaoui, O. Dynamic sorption of methylene blue by cedar sawdust and crushed brick in fixed bed columns. *J. Hazard. Mater.* **2006**, *38* (2), 293–303.

(3) Ajji, Z.; Ali, A. M. Adsorption of methyl violet and brilliant blue onto poly(vinyl alcohol) membranes grafted with N-vinyl imidazole/acrylic acid. *Nucl. Instrum. Methods Phys. Res., Sect. B* **2007**, *265*, 362–365.

(4) Mishra, G.; Tripathy, M. A critical review of the treatment for decolorization of textile effluent. *Colourage* **1993**, *40*, 35–38.

(5) El-Halwany, M. M. Study of adsorption isotherms and kinetic models for Methylene Blue adsorption on activated carbon developed from Egyptian rice hull (Part II). *Desalination* **2010**, *250*, 208–213.

(6) Ofomaja, A. E.; Ho, Y. S. Effect of temperatures and pH on methyl violet biosorption by Mansonia wood sawdust. *Bioresour. Technol.* **2008**, *99*, 5411–5417.

(7) El Mouzdahir, Y.; Elmchaouri, A.; Mahboub, R.; Gil, A.; Korili, S. A. Adsorption of Methylene Blue from Aqueous Solutions on a Moroccan Clay. *J. Chem. Eng. Data* **2007**, *52*, 1621–1625.

(8) Zolgharnein, J.; Shahmoradi, A. Adsorption of Cr(VI) onto *Elaeagnus* Tree Leaves: Statistical Optimization, Equilibrium Modeling, and Kinetic Studies. *J. Chem. Eng. Data* **2010**, *55*, 3428–3437.

(9) Sharma, Y. C.; Uma; Sinha, A. S. K.; Upadhyay, S. N. Characterization and Adsorption Studies of *Cocos nucifera L.* Activated Carbon for the Removal of Methylene Blue from Aqueous Solutions. *J. Chem. Eng. Data* **2010**, *55*, 2662–2667.

(10) Fetterolf, M. L.; Patel, H. V.; Jennings, J. M. Adsorption of Methylene Blue and Acid Blue 40 on Titania from Aqueous Solution. *J. Chem. Eng. Data* **2003**, *48*, 831–835.

(11) Karadag, D.; Turan, M.; Akgul, E.; Tok, S.; Faki, A. Adsorption Equilibrium and Kinetics of Reactive Black 5 and Reactive Red 239 in Aqueous Solution onto Surfactant-Modified Zeolite. *J. Chem. Eng. Data* **2007**, *52*, 1615–1620.

(12) Srivastava, V. C.; Mall, I. D.; Mishra, I. M. Equilibrium Modeling of Ternary Adsorption of Metal Ions onto Rice Husk Ash. *J. Chem. Eng. Data* **2009**, *54*, 705–711.

(13) Wu, Y.; Zhang, L.; Gao, C.; Ma, J.; Ma, X.; Han, R. Adsorption of Copper Ions and Methylene Blue in a Single and Binary System on Wheat Straw. *J. Chem. Eng. Data* **2009**, *54*, 3229–3234.

(14) Hasar, H. Adsorption of nickel (II) from aqueous solution onto activated carbon prepared from almond husk. *J. Hazard. Mater.* **2003**, *97* (1−3), 49–57.

(15) Anonim. Kuru ve Sert Kabuklu Meyveler Dış Pazar Araştırması. İhracatı Geliştirme Etüt Merkezi. Ankara 2000.

(16) Ozdes, D.; Gundogdu, A.; Duran, C.; Senturk, H. B. Evaluation of Adsorption Characteristics of Malachite Green onto Almond Shell (*Prunus dulcis*). *Sep. Sci. Technol.* **2010**, *45*, 2076–2085.

(17) Senturk, H. B.; Ozdes, D.; Duran, C. Biosorption of Rhodamine 6G from aqueous solutions onto almond shell (*Prunus dulcis*) as a low cost biosorbent. *Desalination* **2010**, *252*, 81–87.

(18) Bulut, Y.; Tez, Z. Adsorption studies on ground shells of hazelnut and almond. *J. Hazard. Mater.* **2007**, *149*, 35–41.

(19) Boehm, H. P. Surface oxides on carbon and their analysis: a critical assessment. *Carbon* **2002**, *40*, 145–149.

(20) *APHA, Standard Methods for the Examination of Water and Wastewater*, 18th ed.; American Public Health Association: Washington, DC, 1985.

(21) Alkan, M.; Dogan, M.; Turhan, Y.; Demirbas, Ö.; Turan, P. Adsorption kinetics and mechanism of maxilon blue 5G dye on sepiolite from aqueous solutions. *Chem. Eng. J.* **2008**, *139*, 213–223.

(22) Kumar, K. V.; Sivanesan, S.; Ramamurthi, V. Adsorption of malachite green onto *Pithophora* sp., a fresh water algae: Equilibrium and kinetic modeling. *Process Biochem.* **2005**, *40*, 2865–2872.

(23) Lagergren, S. About the theory of so-called adsorption of soluble substance. *Kung Sven. Veten. Hand* **1898**, *24*, 1–39.

(24) Ho, Y. S.; McKay, G. Kinetic models for the sorption of dye from aqueous solution by wood. *J. Environ. Sci. Health Part B: Process Saf. Environ. Prot.* **1998**, *76* (4), 183–191.

(25) Cheung, C. W.; Porter, J. F.; McKay, G. Sorption kinetic analysis for the removal of cadmium ions from effluents using bone char. *Water Res.* **2001**, *35*, 605–612.

(26) Ncibi, M. C.; Mahjoub, B.; Seffen, M. Kinetic and equilibrium studies of methylene blue biosorption by *Posidonia oceanica (L.)* fibers. *J. Hazard. Mater. B* **2007**, *139*, 280–285.

(27) Weber, W. J., Jr; Morriss, J. C. Kinetics of adsorption on carbon from solution. *J. Sanitary Eng. Div. Am. Soc. Civ. Eng.* **1963**, *89*, 31–60.

(28) Hameed, B. H.; El-Khaiary, M. I. Kinetics and equilibrium studies of malachite green adsorption on rice straw-derived char. *J. Hazard. Mater.* **2008**, *153*, 701–708.

(29) Cheng, W.; Wang, S. G.; Lu, L.; Gong, W. X.; Liu, X. W.; Gao, B. Y.; Zhang, H. Y. Removal of malachite green (MG) from aqueous solutions by native and heat-treated anaerobic granular sludge. *Biochem. Eng. J.* **2008**, *39*, 538–546.

(30) Sharma, P.; Kaur, R.; Baskar, C.; Chung, W. J. Removal of methylene blue from aqueous waste using rice husk and rice husk ash. *Desalination* **2010**, *259*, 249–257.

(31) Langmuir, I. The adsorption of gases on plane surfaces of glass, mica and platinum. *J. Am. Chem. Soc.* **1918**, *40*, 1361–1403.

(32) Weber, T. W.; Chakravorti, P. K. Pore and solid diffusion models for fixed bed adsorbent. *J. Am. Inst. Chem., Engrs.* **1974**, *20*, 228–252.

(33) Freundlich, H. M. F. Über die adsorption in lösungen. *Z. Phys. Chem.* **1906**, *57*, 385–470.

(34) Temkin, M. J.; Pyzhev, V. Recent modifications to Langmuir isotherms. *Acta Physiochim. USSR* **1940**, *12*, 217–222.

(35) Dubinin, M. M.; Radushkevich, L. V. Equation of the characteristics curve of activated charcoal. *Chem. Zent.* **1947**, *1*, 875.

(36) Helfferich, F. *Ion Exchange*; McGraw-Hill: New York, 1962.

(37) Azizian, S.; Haerifar, M.; Bashiri, H. Adsorption of methyl violet onto granular activated carbon: Equilibrium, kinetics and modeling. *Chem. Eng. J.* **2009**, *146*, 36–41.

(38) Mall, I. D.; Srivastava, V. C.; Agarwal, N. K. Removal of Orange-G and Methyl Violet dyes by adsorption onto bagasse fly ash-kinetic study and equilibrium isotherm analyses. *Dyes Pigments* **2006**, *69*, 210–223.

(39) Vadivelan, V.; Kumar, K. V. Equilibrium, kinetics, mechanism, and process design for the sorption of methylene blue onto rice husk. *J. Colloid Interface Sci.* **2005**, *286*, 90–100.

(40) Bhattacharyya, K. G.; Sharma, A. Kinetics and thermodynamics of methylene blue adsorption on Neem (*Azadirachta indica*) leaf powder. *Dyes Pigments* **2005**, *65*, 51–59.

(41) Kavitha, D.; Namasivayam, C. Experimental and kinetic studies on methylene blue adsorption by coir pith carbon. *Bioresour. Technol.* **2007**, *98*, 14–21.

(42) Yao, Y.; Xu, F.; Chen, M.; Xu, Z.; Zhu, Z. Adsorption behavior of methylene blue on carbon nanotubes. *Bioresour. Technol.* **2010**, *101*, 3040–3046.

(43) Rauf, M. A.; Qadri, S. M.; Ashraf, S.; Al-Mansoori, K. M. Adsorption studies of Toluidine Blue from aqueous solutions onto gypsum. *Chem. Eng. J.* **2009**, *150*, 90–95.

(44) Alpat, S. K.; Özbayrak, Ö.; Alpat, Ş.; Akçay, H. The adsorption kinetics and removal of cationic dye, Toluidine Blue O, from

aqueous solution with Turkish zeolite. *J. Hazard. Mater.* **2008**, *151*, 213–220.

(45) Xiong, L.; Yang, Y.; Mai, J.; Sun, W.; Zhang, C.; Wei, D.; Chen, Q.; Ni, J. Adsorption behavior of methylene blue onto titanate nanotubes. *Chem. Eng. J.* **2010**, *156*, 313–320.

(46) Cengiz, S.; Cavas, L. Removal of methylene blue by invasive marine seaweed: *Caulerpa racemosa* var. *Cylindracea*. *Bioresour. Technol.* **2008**, *99*, 2357–2363.

(47) Smith, J. M., Van Ness, H. C. *Introduction to Chemical Engineering Thermodynamics*, 4th ed.; McGraw-Hill: Singapore, 1987.